



Experimental characterisation of flexural bond behaviour in brick masonry

Maria B. Gaggero · Rita Esposito

Received: 2 July 2022 / Accepted: 2 March 2023 / Published online: 28 March 2023
© The Author(s) 2023

Abstract The brick-to-mortar bond often represents the weakest link leading to cracking and failure of masonry structures. For this reason, the in-situ characterization of masonry's flexural bond behaviour (here defined as flexural bond strength and flexural bond fracture energy), is essential for the assessment of existing buildings. Among masonry bond properties, the flexural bond strength is commonly determined on-site, given the minimal invasiveness of the so-called bond wrench test. However, often the reliability of the results is questioned inputting their large variability to the operator. The present study discharges this assumption by comparing the accuracy of various testing set-ups (manually-operated vs computer-controlled set-ups). Additionally, the influence of the specimen's type (with/without head joints and couplets vs wallet) on the flexural bond strength assessment is studied providing preliminary correlation factors that can be of help for the in-situ measurement on single-wythe masonry. In addition, to obtain a complete description of the bond behaviour, a new test set-up able to determine the post-peak response is presented. Considerations regarding the dissipated bond fracture energy and its

relation to the tensile fracture energy are provided with the support of literature data.

Keywords Brick masonry · Bond wrench test · Flexural bond strength · Tensile behaviour · Fracture energy

List of symbols Roman symbols

b	Length of the mortar bed joint in a masonry specimen
e_1	Distance from the applied load to the tension face of the specimen
f_{bc}	Normalised compressive strength of masonry brick
f_{mt}	Flexural strength of masonry mortar
f_w	Flexural bond strength
A	Cracking area
F_2	Vertical load due to the weight of the top clamping system of the bond wrench apparatus
G_{ft}	Tensile bond fracture energy evaluated through direct tension tests
W	Dissipated energy in a CMOD-controlled bond wrench test
d	Width of the mortar bed joint in a masonry specimen
e_2	Distance from the centre of gravity of the clamp to the tension face of the specimen
f_{mc}	Compressive strength of masonry mortar
f_t	Tensile bond strength

M. B. Gaggero (✉) · R. Esposito
Faculty of Civil Engineering and Geosciences, TU Delft,
Stevinweg 1, 2628 CN Delft, The Netherlands
e-mail: M.B.Gaggero@tudelft.nl

R. Esposito
e-mail: R.Esposito@tudelft.nl



F_1	Applied failure load registered in bond wrench tests
F_3	Vertical load due to the weight of top masonry brick pulled off the specimen
G_{fw}	Flexural bond fracture energy evaluated through flexural type tests

Abbreviations

Avg.	Average
C.o.V.	Coefficient of variation
IRA	Initial rate of absorption
St.dev.	Standard deviation
CMOD	Crack mouth opening displacement
CS	Calcium silicate
LVDT	Linear variable differential transformer

1 Introduction

The brick-to-mortar bond frequently represents the weakest link in masonry structures, governing in many cases their behaviour, e.g. under in-plane and out-of-plane loads induced by wind and earthquakes. An inadequate bond strength inevitably leads to cracking: aesthetic damage and loss of water tightness of the masonry component may occur in the case of low magnitude loads, while potential widespread damages may occur in extreme load events leading to collapse. Hence, a complete in-situ characterisation of the masonry bond behaviour is highly relevant towards the structural assessment of existing buildings and subsequent design of future strengthening and repairing interventions, if needed. This comprehensive description comprises the full anelastic stress-displacement diagram in tension (Mode-I) and shear (Mode-II). Within this framework, the bond wrench test is commonly used for the indirect characterisation of the tensile behaviour due to its minimal invasiveness in determining the flexural bond strength on site.

The bond wrench test is described by international standards as the EN 1052-5:2002 [1] and ASTM C 1072 [2], and was conceived as a control tool to be performed on small masonry specimens, i.e. several-brick high stack-bonded prisms or stack-bonded couplets. It mainly consists of applying an increasing eccentric load to a single brick–mortar interface by using a lever arm clamped to the top brick of the specimen. The potential of such a procedure lies in its simplicity, being a reliable quick-to-implement

alternative to laborious bending tests performed on relatively big specimens, namely wallets. As a matter of fact, multiple comparative experimental studies have confirmed the reliability of its outcome, reporting a one-to-one correspondence with four-point bending test results [3–5]. As for other bending tests, the resulting flexural bond strength is calculated by considering a fictitious linear stress distribution at failure and must be then adjusted by a correction factor to obtain the tensile bond strength. This correction factor was identified by many authors and is generally assumed to be 1.5 [6]. Given the potentiality pointed out and the applicability of the testing method to in-situ applications, further research has been conducted to investigate correlations between the provided flexural bond strength and other mechanical properties of the masonry. In particular, the work performed by Jafari [3] summarised the utility of performing in-situ bond wrench tests for the indirect estimation of the flexural bond strength perpendicular to the bed joint and the mortar compressive strength, in addition to the aforementioned tensile bond strength.

Although its potentiality, bond wrench tests often provide large coefficient of variation ranging between 15 and 50% even in controlled laboratory conditions [7]. This variability is predominant for cases of poorly bonded masonry, such as historical masonry and masonry subjected to deterioration. Whether this variability is attributed exclusively to the natural variations in the material's properties or partially due to the accuracy of the testing set-up is a research question still open. In fact, masonry bond is known for being strongly dependent on the brick's absorption properties and the composition, water retentivity and initial flow of the mortar [8–10]. The natural variation of these factors within and between batches, can result in a bond variability that could be considered an intrinsic property of masonry. Nonetheless, the high variability for in-situ measurements is often attributed to the user. As a matter of fact, in the commonly used manually-operated set-up, the load rate cannot be controlled and specimens of the same set might not be tested identically. However, limited information about the influence of the accuracy of bond wrench test set-ups upon the measured variability is available in literature [4, 11]. In addition, the information available mainly regards tests performed on stack-bonded couplets or prisms, which are different from those used for in-situ testing, where masonry courses



arranged with non-stacked bond pattern are tested. Whether the bond strength obtained from standard specimens (stack-bonded couplets or prism) agreed with the one obtained from the entire wall is, in fact, another important point that still lacks insight. From the experimental program performed by Correa et al. [12] on 6-bricks high stack-bonded prisms and full-sized walls made of solid clay brick masonry, no consistent relationship between the two types of specimens has been observed. Finding the prism's mean flexural bond strength higher than the walls' mean strength, the author suggested that several-brick high stack-bonded prisms do not accurately represent the joints within a wall. The highlighted lack of correlation was attributed to the different level of disturbance that may occur in the two types of specimens during construction. In fact, several-brick high stack-bonded prisms are built by stacking bricks on top of each other while the mortar is still fresh: movements of the higher bricks and their weight may disturb the joints below. Unlike, joints in walls remain undisturbed until the corresponding course is completed. Therefore, the author suggested further investigating the implementation of a specimen's type that may better represent the level of disturbance of a bed joint within a wall while being constructed, such as masonry couplets. However, this aspect has not been studied in literature yet.

Besides the high variability observed in bond wrench test results, the commonly implemented force-controlled set-up is inadequate to measure the post-peak softening response of masonry bond. This information would give an indication of the energy dissipated during the test, hereafter referred to as flexural bond fracture energy, which could be associated with the tensile bond fracture energy. Defined as the amount of energy per unit of area required for creating a crack along the brick-to-mortar interface, the tensile bond fracture energy is calculated as the area underneath the stress-displacement diagram in the post-peak softening branch. Its determination is required to describe the quasi-brittle response of masonry or predict masonry's cracking and failure process through nonlinear analysis. In this context, a small variation of the tensile bond fracture energy may lead to a variation in the estimation of, e.g., the out-of-plane force capacity [13, 14] and the in-plane capacity in terms of ductility and base shear force [15] of masonry walls, and the crack width and damage level

of masonry buildings [16]. However, this property is never tested in-situ when performing structural assessments. Instead, it is generally adopted relying on limited experimental results, e.g. Barros et al. [17] and Van der Pluijm [18], or representative values provided by guidelines [19], which may not be valid for all masonry types and conditions. Given the complexity of its experimental assessment through direct tensile tests, flexural type tests may substitute, as it is common for other materials [20]. Nevertheless, this for masonry is up today not done. In this context, laboratory bond wrench tests could represent a solution if an improved deformation-controlled set-up is introduced. Since controlling in-situ tests would be nearly impossible, a reliable correlation between the flexural bond strength and flexural bond fracture energy would also be needed for its indirect estimation in in-situ applications.

This paper aims to explore the experimental characterisation of masonry bond behaviour with the bond wrench tests as a means to accurately predict both the flexural bond strength and flexural fracture energy on-site or on field-extracted sample. In this context, the effect on the flexural bond strength assessment of the set-up's accuracy and specimen type was investigated in response to its high variability and the lack of correlation between standard specimens used in laboratory tests (i.e. stacked bonded couplets) and the ones usually tested in-situ (with head joint and courses). Additionally, the set-up's applicability to measure the flexural bond fracture energy and indirectly estimate the tensile bond fracture energy was studied with the support of available literature data.

2 Materials and methods

The purpose of the experimental program was to analyse the effect of different set-ups and different specimen's types on the flexural bond strength assessment performed through the bond wrench test. Among the set-ups considered, the research of a procedure to evaluate the post-peak behaviour and assess the flexural bond fracture energy was also aimed. The study focused on unreinforced brick masonry, mainly single width. In particular, tests were carried out on poorly bonded masonry specimens showing a high coefficient of variation in bond wrench

tests. Calcium silicate (CS) brick masonry with a cement-based mortar and clay brick masonry with a cement-lime mortar, replicated to mimic the mechanical properties of samples extracted from existing buildings [21], were used. The same masonry types have been used in an extensive multi-scale experimental campaign to support the assessment of Dutch buildings subject to induced seismicity [22]. For a complete overview of the characterisation of both types of masonry, the reader is referred to Jafari [3]. Please note that the materials used (bricks and mortar) in the present research and in the one by Jafari [3] were manufactured in the same production batch, stored in closed space at room temperature, and assembled with the same procedure during the different construction periods.

Traditional CS and clay bricks were used. Their nominal dimension, compressive strength (f_{bc}) and initial rate of absorption (IRA) were reported in Table 1. The reported compressive strength was determined by Jafari [3] accordingly to EN 772-1 [23]. The IRA was herein determined in accordance with EN 772-1 [24] to compare, due to the influence of absorption properties on the flexural bond strength assessment, the results of both types of masonry.

The mortars used were a 1:3 (cement: sand proportions by volume) cement-based mortar and a 1:2:9 (cement: lime: sand proportions by volume) cement-lime mortar. Many different mortar batches have been used to build masonry specimens mainly in two constructions periods, i.e. August 2018 and February 2019. In each batch produced within the experimental campaign the initial flow of fresh mortar and the compressive and flexural strength of hardened mortar (f_{mc} and f_{mt} respectively) was evaluated in accordance with EN 1015-3 [25] and EN 1015-11 [26] respectively. In February 2019, the aforementioned mechanical properties have been evaluated not only at an age of 28 days as prescribed in the standard, but also at 14 and 56 days. The results for both mortar

compositions are summarized in Table 2, including the construction period and the specimen's type built within the single batch.

Masonry specimens built within the presented experimental campaign had a 10-mm mortar joint and were built in controlled laboratory conditions by a professional bricklayer. Bricks were not pre-wet prior to use, and no weight was placed on the specimens right after construction to be consistent with Jafari [21] and replicate poorly bonded masonries. After construction all specimens were cured at room temperature and tested at different ages.

To investigate whether the set-up influences the flexural bond strength assessment, three standardized set-up variants have been implemented on “standard” couplets prescribed in EN 1052-5 [1]. The force-controlled set-up widely used for laboratory testing in previous experimental campaigns performed at the Delft University of Technology [3] was considered the starting point for the design process of the other two apparatus. In such a conventional set-up (Fig. 1a), the user operates the jack by slowly turning a crank, which means that human interaction is required to apply the load. The design of a more sophisticated, computer-controlled set-up operated by controlling the crack mouth opening displacement (CMOD) at the tension side of the tested specimen took place to investigate whether removing the human factor reduces the variability of bond wrench data (Fig. 1b). The CMOD-controlled procedure implemented allows capturing the material's post-peak behaviour and evaluating the flexural bond fracture energy. However, since both the configurations above are non-portable and exclusively suitable for laboratory testing, a more simplified and portable, force-controlled bond-wrench apparatus operated entirely by hand has been designed (Fig. 1c, d). In this latter case, the user applies the load by pressing a torque wrench, and therefore the degree of human interaction is even higher than in the conventional set-up.

Table 1 Overview of the physical and mechanical properties of the bricks used

Brick type	Brick size Length × height × thickness (mm ³)	f_{bc} [3]			IRA		
		No. test	Avg. (MPa)	C.o.V. (%)	No. test	Avg. (kg/m ²)	C.o.V. (%)
CS	210 × 70 × 100	6	13.3	13	6	1.0	10
Clay	210 × 50 × 100	9	28.3	10	6	3.3	12



Table 2 Overview of the physical and mechanical properties of the mortar within the experimental campaign

Brick-mortar ^a type	Construction period	Specimen's type	Mortar flow (mm)	Hardening time (days)	f_{mc}		f_{mt}	
					No. test	Avg. (MPa)	No. test	Avg. (MPa)
CS—1:3 (cement:sand)	2018	Stack-bonded couplets, running-bonded wallets	161	30	6	5.4 (3)	3	2.4 (7)
	2019	Stack-bonded couplets, running-bonded couplets	160	14	6	5.3 (6)	3	0.7 (4)
				28	6	5.3 (5)	3	2.4 (5)
Clay—1:2:9 (cement:lime:sand)	2018	Stack-bonded couplets, running-bonded wallets	183	31	6	3.2 (16)	2	1.6 (6)
				2019	Stack-bonded couplets, running-bonded couplets	193	14	6
	28	6	3.7 (5)				3	1.4 (2)
					56	6	4.2 (4)	3

The coefficient of variation of each series is reported in brackets

^aMortar composition by volume ratio

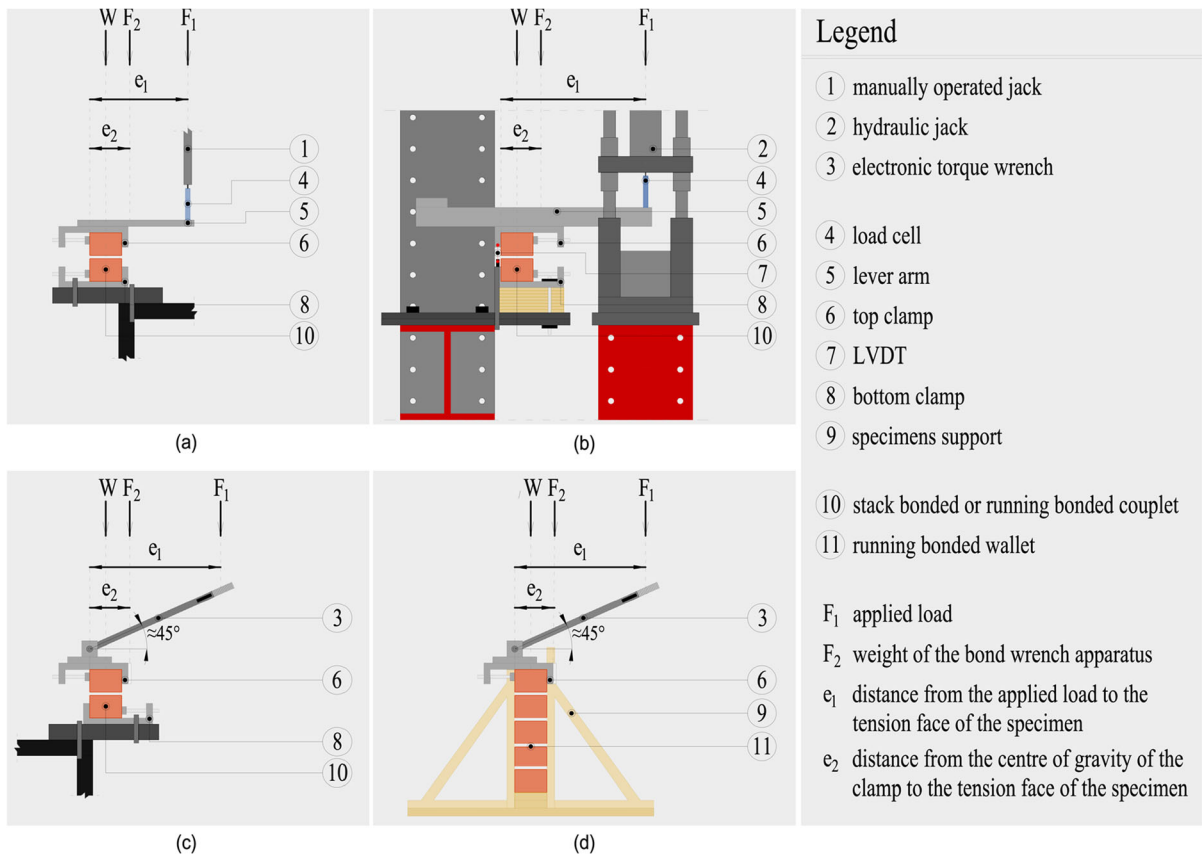


Fig. 1 a Force-controlled and b CMOD-controlled set-up for laboratory tests on couplets. Set-up for in-situ tests on c couplets and d wallets [28]

In addition to “standard”, stack-bonded couplets (Fig. 2a), the in-situ set-up has also been carried out on two additional types of masonry specimens to investigate the influence of the specimen’s type on the flexural bond strength assessment. Running-bonded couplets (Fig. 2b) and running-bonded wallets (Fig. 2c) have been considered to correlate laboratory testing generally performed on “standard”, stack-bonded couplets and in-situ testing performed on portions of masonry. The bond wrench test was performed on the remaining intact parts of running-bonded wallets slightly damaged (not until failure) in previous 4-point bending tests [27]; the exact location of the damage was known due to the use of Digital Image Correlation (DIC) [28].

For each test, the standard EN 1052-5:2002 [1] was used as a guideline to design the testing procedure. A support frame, composed of a bottom screw clamp firmly gripped to a base frame, was used to restrain the lower brick of both types of couplets (Fig. 1a, b, c). Conversely, running-bonded wallets were rigidly held in place by a wooden support frame (Fig. 1d); the brick–mortar interface under test was isolated before testing, cutting the head joints with a hacksaw. A lever arm directly connected to a clamp that holds the top brick applied a bending moment to the brick–mortar interface. The same bottom and top clamp were used

in the three set-ups, while the lever arm changed. The set-ups for laboratory tests employed a 100 kN jack to apply the vertical load at the free end of the lever arm and a load cell with accuracy ± 1 N for its measurement. While in the conventional set-up a mechanical jack operated manually was used, in the CMOD-controlled set-up a hydraulic jack operated in displacement-controlled was adopted. In this latter case, the control variable used was the average displacement measured by two LVDTs (measuring range within ± 1 mm, accuracy of ± 0.01 mm) attached to the upper clamp to register relative vertical displacements with respect to the bottom clamp (Fig. 1b). In particular, the applied displacement rate, experimentally determined as the fastest value that allowed measuring the post-peak behaviour of both types of masonry, was 0.001 mm/s and 0.002 mm/s for CS and solid clay specimens, respectively. As an alternative to both laboratory set-ups, the configuration for in-situ testing employed an electronic torque wrench in which a digital display showing the applied failure load with an accuracy of $\pm 2\%$ reading. Based on previous bond-wrench test results [3], two electronic torque wrenches with a different measurement range were used to test each type of masonry: 10–100 Nm and 40–400 Nm for clay and CS specimens, respectively.

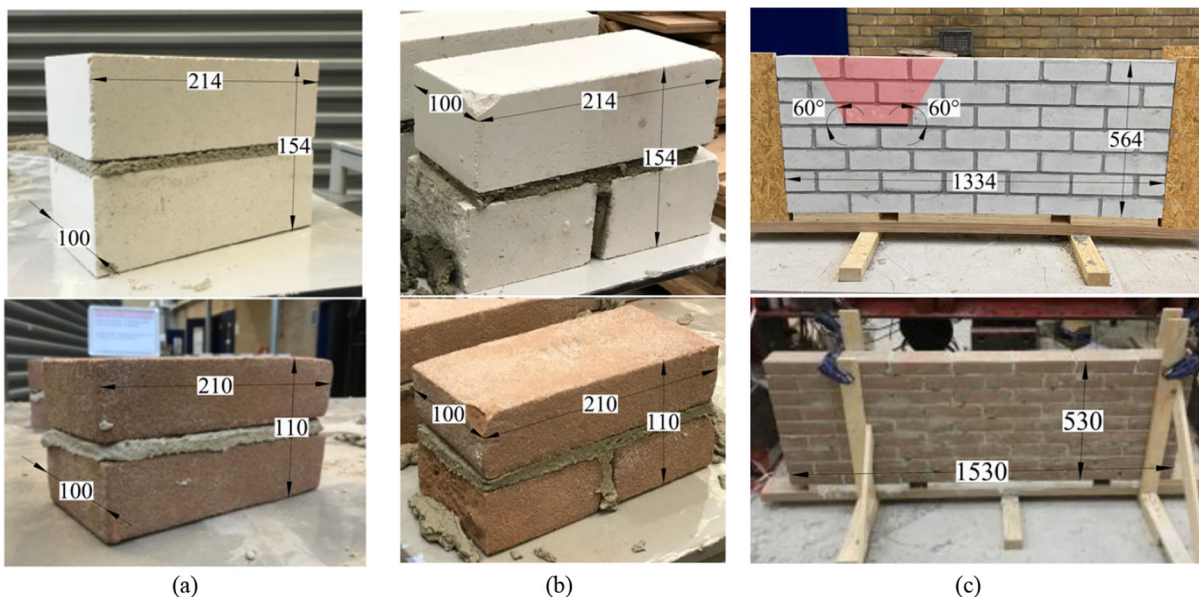


Fig. 2 Specimen’s type considered in the experimental study: **a** stack-bonded couplets, **b** running-bonded couplets and **c** running-bonded wallets

The flexural bond strength of masonry specimens was calculated, in accordance with the EN 1052-5:2002 [1] with the following formula:

$$f_{w,i} = \frac{F_1 + F_2 e_2 - \frac{2}{3} d (F_1 + F_2 + \frac{W}{4})}{\frac{bd^2}{6}} \quad (1)$$

where F_1 is the failure load registered during the test by the load cell in both laboratory set-ups or by the electronic torque wrench in the in-situ configuration, F_2 is the normal force as a result of the weight of the bond wrench apparatus, F_3 is the weight of the masonry brick pulled off the specimen and any adherent mortar, e_1 is the distance from the applied load to the tension face of the specimen, e_2 is the distance from the centre of gravity of the clamp to the tension face of the specimen and b and d is the mean length of the bed joint and the mean width of the bed joint respectively. The values assumed by the aforementioned parameters in each configuration are listed in Table 3. The set-up is described by the test condition (lab or in-situ), the control parameter (force or CMOD) and test operability (by hand or computer).

In addition, the CMOD-controlled set-up allowed determining the post-peak behaviour of the material and consequently the amount of energy dissipated due to the joint cracking. Figure 3 shows an example of measured data in terms of clamp opening measured by the LVDTs and in terms of vertical displacement of the jack. To calculate the amount of dissipated energy (W), the area underneath the force versus vertical displacement of the jack is considered. By considering as fracture surface (A) the cross-section of the tested interface, the flexural bond fracture energy (G_{fw}) is calculated as follows:

$$G_{fw} = \frac{W}{A} \quad (2)$$

In Table 4, an overview of the experimental campaign is presented. The specimen tested in each

series is identified by specifying the type, the construction year and the testing age.

3 Experimental results

The flexural bond strength of all tests performed and, where feasible, also the flexural bond fracture energy, are listed by masonry and test type in Table 5. All tests performed led to bond failure at the interface between brick and mortar. For this reason, in this paper, only bond type properties are considered.

Regardless of the test set-up, in several cases failure during the installation of clay masonry specimens was observed, attributing a null flexural strength value to these specimens. Notably, the set of stack-bonded couplets cast in 2019 and tested at 14 days with the CMOD-controlled set up for laboratory testing, where ten out of ten specimens failed during their installation, and consequently, null flexural bond strength and null flexural bond fracture energy values have been reported.

Comparing both types of brick masonry, it can be observed that the bond of calcium silicate (CS) masonry is four times stronger than one of clay masonry. The weakness of clay masonry bond can be attributed to the high IRA values of bricks (3.3 kg/m^2): the process of water suction from the mortar when the brick is placed is significantly fast, generating a dry, weak interface. This result was expected since pre-wetting of the brick was not implemented prior to construction to achieve low bond values similar to the one observed for existing buildings [21].

In addition, the coefficient of variation obtained for clay brick masonry resulted two times higher than the one for CS masonry, although similar values of standard deviation are reported. In fact, it is the mean flexural bond strength that has more influence on the coefficient of variation. Consequently, stronger

Table 3 Set-up parameters employed in the flexural bond strength calculation

Test condition	Control parameter	Test operability	Masonry type	e_1 (mm)	e_2 (mm)	F_2 (N)
Lab	Force	By hand	CS and clay	500.0	51.0	50.9
	CMOD	Computer	CS and clay	460.0	53.1	85.0
In-situ	Force	By hand	CS	630.0	55.3	106.4
			Clay	480.0	34.5	110.6

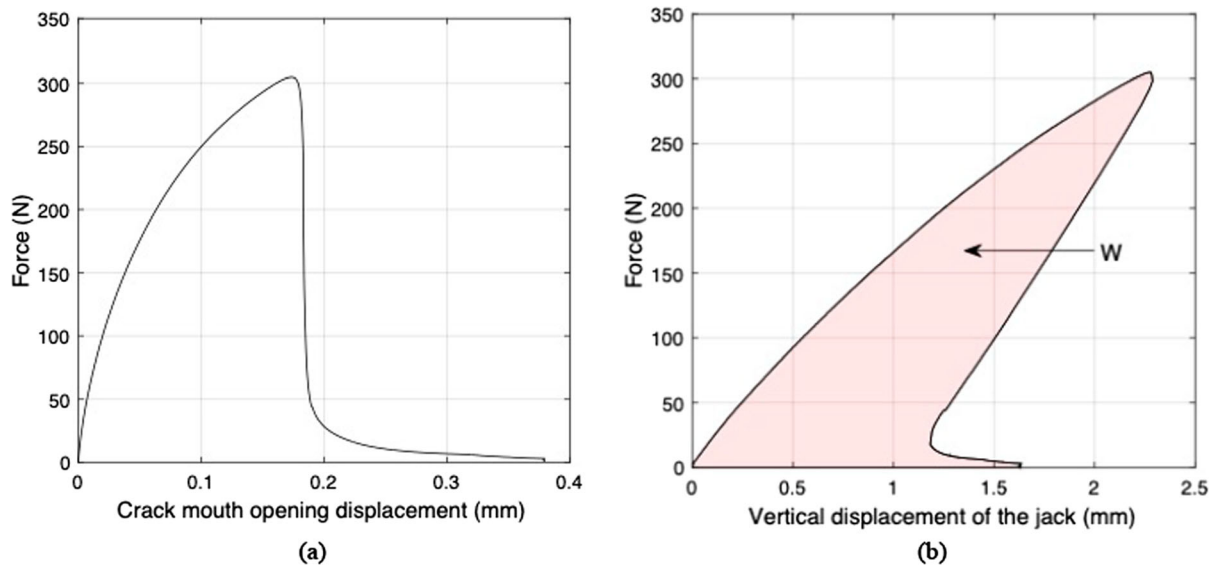


Fig. 3 Example of measured data with the CMOD-controlled bond wrench test set-up: applied force as a function of **a** CMOD and **b** vertical displacement of the jack

Table 4 Overview of the experimental campaign

Masonry type	Test condition	Control parameter	Test operability	Specimen's type	Construction period (year)	Hardening time (days)	
CS	Lab	Force	By hand	Stack-bonded couplets	2018	37	
					2018	100	
		CMOD	Computer	Stack-bonded couplets	2018	188	
					2019	14	
					2019	28	
	In-situ	Force	By hand	Stack-bonded couplets	2018	132	
					Running-bonded couplets	2019	56
Clay	Lab	Force	By hand	Stack-bonded couplets	2018	42	
					2018	145	
		CMOD	Computer	Stack-bonded couplets	2018	197	
					2019	14	
					2019	28	
	In-situ	Force	By hand	Stack-bonded couplets	2018	125	
					Running-bonded couplets	2019	56
					Running-bonded wallet	2018	145
					Running-bonded wallet	2018	145

Table 5 Value of flexural bond strength f_w and flexural bond fracture energy G_{fw} obtained in the experimental campaign

Masonry type	Test condition	Control parameter	Specimen's type	Construction period (year)	Hardening time (days)	No. tests (-)	f_w		G_{fw}		
							Avg. (N/mm)	St.dev. (N/mm)	Avg. (N/mm)	St.dev. (N/mm)	
CS	Lab	Force	Stack-bonded couples	2018	37	10	0.45	0.07	—	—	—
				2018	100	5	0.45	0.03	—	—	—
				2018	188	10	0.33	0.02	0.017	0.008	46
				2019	14	10	0.35	0.08	0.021	0.009	45
				2019	28	10	0.36	0.11	0.023	0.014	61
	In-situ	Force	Running-bonded couples	2018	56	10	0.36	0.04	0.022	0.01	46
				2018	132	10	0.36	0.03	—	—	—
				2019	56	8	0.42	0.05	—	—	—
				2018	145	22	0.54	0.08	—	—	—
				2018	42	10	0.09	0.03	—	—	—
Clay	Lab	Force	Stack-bonded couples	2018	197	9	0.14	0.05	0.012	0.011	86
				2019	14	10	0	—	0	—	—
				2019	28	8	0.07	0.03	0.002	0.001	59
				2019	56	6	0.09	0.04	0.005	0.004	89
				2018	125	13	0.12	0.04	—	—	—
	In-situ	Force	Running-bonded couples	2019	56	2	0.25	0.07	—	—	—
				2018	145	18	0.26	0.07	—	—	—
				2018	—	—	—	—	—	—	—
				2018	—	—	—	—	—	—	—
				2018	—	—	—	—	—	—	—



bonded masonry as CS gives a seemingly lower variability overall than poorly bonded masonry as clay.

4 Influence of the test set-up

To evaluate the influence of the set-up's accuracy on bond wrench test results, the outcome of the three proposed configurations performed on "standard" couplets are compared. Since tests were performed at different maturation days to fit the construction of each set-up in between testing, the combined effect of set-up and hardening time is herein examined. Figure 4a and b show the flexural bond strength against the hardening time of calcium silicate (CS) and clay couplets, respectively. For both masonry types considered, results are grouped by construction period

(2018 or 2019) and set-up. Blue and orange markers are used respectively for the force-controlled and CMOD-controlled set-up proposed for laboratory tests, while green markers are used for the in-situ configuration. The average flexural bond strength of each series is highlighted with a filled marker, and the relative C.o.V is also reported.

Comparing the variability within data sets obtained with the three testing configurations on couplets cast in 2018, no influence of the accuracy of the control is observed. In fact, a similar coefficient of variation, namely 7%–16% for CS (Fig. 4a) and 34–39% for clay (Fig. 4b), is reported independently from the set-up. Regardless of the masonry type considered in Fig. 4, the variability resulted slightly lower for specimens tested at later ages, in which the bond development is expected to be achieved completely. On the other hand, the difference in terms of average can be

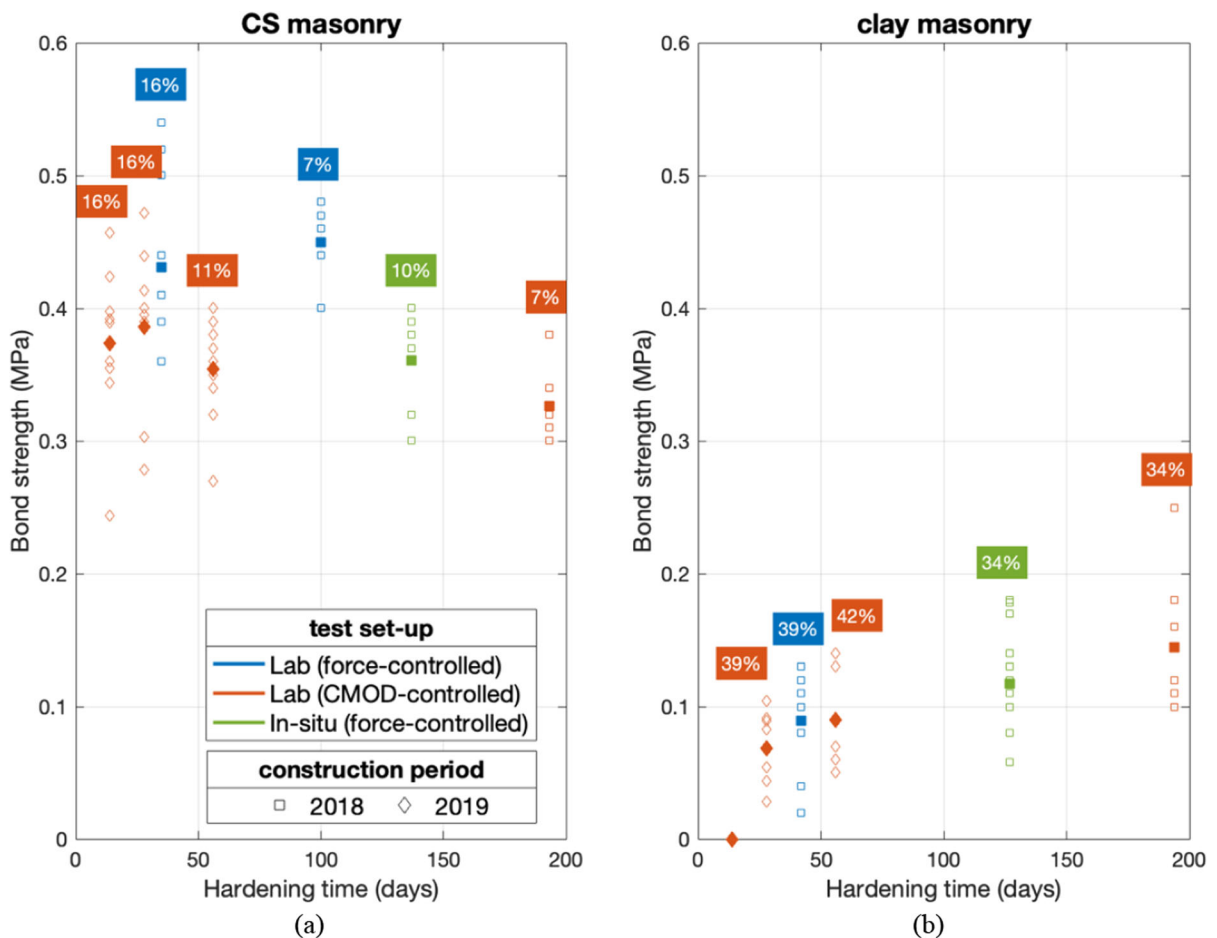


Fig. 4 Flexural bond strength obtained on stack-bonded couplets with different bond wrench test set-ups as a function of time



attributed to the effect of hardening time and not to the set-up implemented.

To highlight the influence of hardening time, the data set is expanded with the results obtained in 2019. On the one hand, the long-term flexural bond strength increase observed in Fig. 4b for clay specimens can be attributed to the presence of lime in the mortar composition. Unlike cement-based mortar, lime carbonation is a slower hardening process that might take years to conclude. On the other hand, the decreasing trend over time observed in Fig. 4a for CS specimens could be attributed to shrinkage phenomena of the material itself. Factors influencing long-term bond strength, such as the lime carbonation (Fig. 4b) and mortar drying shrinkage (Fig. 4a), have been highlighted by many authors, as reported by Sugo et al. [29].

5 Influence of the specimen's type

To evaluate the influence of the specimen's type on the flexural bond strength assessment, results obtained with the in-situ set-up on stack-bonded couplets, running-bonded couplets and running-bonded wallets is compared. Figure 5a and b show the results of calcium silicate (CS) and clay specimens, respectively. In both cases, the obtained flexural bond strength is reported as a function of the initial normal stresses caused by the self-weight of the masonry portion situated above the tested bed joint. In particular, the pre-compression was calculated in the intact version of the specimen, i.e. after construction and before testing, considering the masonry within a conical angle of 60 degrees (Fig. 2c). The latter assumption was made based on how concentrated loads may be spread along a masonry wall, referring to Eurocode 6 [30]. In the calculation, a masonry's density of 1763 kg/m³ and 1708 kg/m³ was considered for CS and clay brick masonry, respectively. The exposed representation allows examining whether there exists a trend of results according to the position of the tested bed joint within a wall. In particular, green markers indicate the average flexural strength obtained for stack-bonded couplets and blue markers refer to running-bonded couplets. In the case of running-bonded wallets, results are illustrated by the values for each bed joint tested (grey markers), the average strength per course (red markers), the average

strength considering all courses for the running-bonded wallet and the relative standard deviation (continuous red line and dashed grey line respectively). Table 6 lists the average flexural bond strength value obtained for the three specimens and their ratio with respect to the value obtained by tests on stack-bonded specimens. As for running-bonded wallets, the results mentioned above are reported for the first course and for the overall specimen considering all the courses.

Comparing the results obtained on stack-bonded couplets and running-bonded wallets, the former shows lower flexural bond strength for both masonry types. Contrary to the results obtained by Correa et al. [12] on 6-brick high stack-bonded prisms, stack-bonded couplets led to a conservative estimation of the wallet bond. Therefore, the implementation of stack-bonded couplets might be better for design or control purposes than several-brick high prisms. In particular, a 1.5 and 2.2 factor was obtained respectively for CS (Fig. 5a) and clay (Fig. 5b) masonry, as reported in Table 6. Regardless of the type of masonry considered, the latter may probably be attributed either to the pre-compression level caused by the self-weight or to the presence of head joints which could modify the specimen drying process. Regarding the pre-compression level, no particular trend in the flexural bond strength versus pre-compression graph is observed within the wallet (Fig. 5a, b). In addition, a difference between the average of the bed joint tested in the first course of running-bonded wallets and the result of stack-bonded couplets is also observed, even if the pre-compression stress value was the same. These findings are consistent with the work of De Vekey et al. [7], where bond wrench measurements from existing buildings showed no influence of the position of the tested joint within walls. This lack of spatial correlation, also highlighted by Correa et al. [12] and Heffler et al. [31], would suggest that testing specimens subjected to low or high axial pre-compression stresses should lead to the same result, making the selection of the portion of the wall to be tested less restrictive in in-situ applications. Nevertheless, such a consideration is possible only if the conditions on each joint along the height of the wall is the same, e.g. filling of the joint.

Hence, the flexural bond strength of bed joints is probably influenced by the presence of head joints. However, by considering running-bonded couplets, it

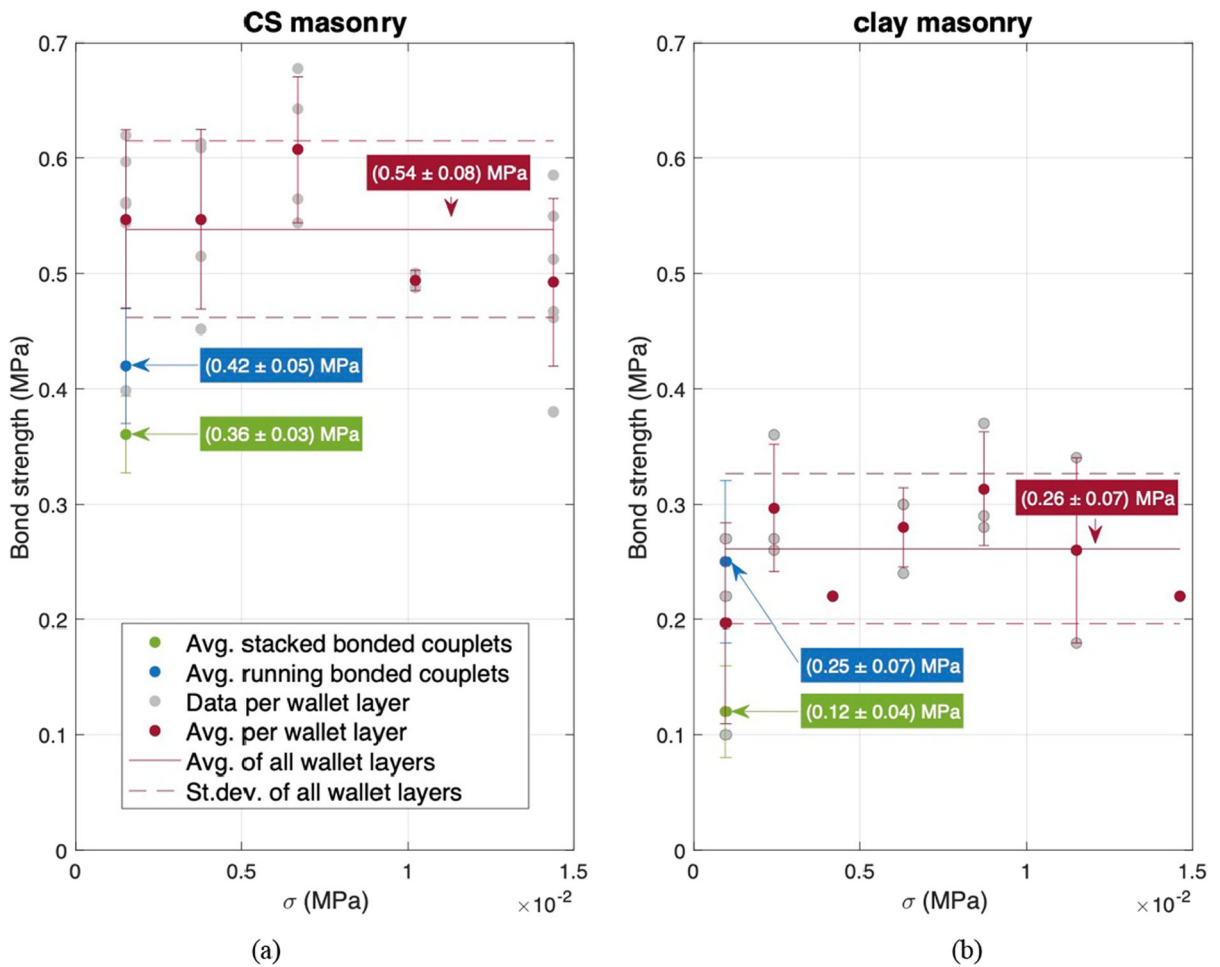


Fig. 5 Flexural bond strength as a function of pre-compression: **a** CS masonry; **b** clay masonry

Table 6 Differences between the results obtained with the in-situ set-up on the three proposed specimen’s types

Index (i)	Specimen’s type	CS				Clay			
		No. test	Avg. f_w (MPa)	C.o.V. f_w (%)	Ratio f_w (i)/(1)	No. test	Avg. f_w (MPa)	C.o.V. f_w (%)	Ratio f_w (i)/(1)
(1)	Stack-bonded couplet	10	0.36	9	1	13	0.12	35	1
(2)	Running-bonded couplet	8	0.42	11	1.2	2	0.25	25	2.1
(3)	Running-bonded wallet— all courses	23	0.54	14	1.5	18	0.26	27	2.2
(4)	Running-bonded wallet— first course	6	0.55	8	1.5	3	0.20	9	1.6

is not possible to obtain a clear indication of the influence of the head joint on the flexural bond strength of bed joints. For CS (Fig. 5a), the difference in terms of flexural strength between running-bonded

wallets and running-bonded couplets is similar to the one obtained between running-bonded wallets and stack-bonded couplets. Conversely, for clay brick masonry (Fig. 5b), the running-bonded couplets



provide similar results to the running-bonded wallets. However, these considerations may not be statistically valid due to the limited number of specimens tested.

6 Bond fracture energy: flexural type versus direct tensile tests

The characterisation of the masonry's softening behaviour in tension is of importance for the assessment of existing masonry structures, as shown for example in [13–16]. However, direct tensile tests are challenging and often are not commonly available in laboratory [32]. This increase the assumptions on this parameter that cannot be tested. It is thus of relevance to investigate whether the use of bending type tests can indirectly lead to an estimation of the tensile bond fracture energy. In this respect, the new CMOD-controlled set-up proposed here is adopted to estimate the flexural bond fracture energy. By gathering of literature data, preliminary considerations on the relation of flexural and tensile bond fracture energy are made.

Figure 6 illustrates the average bond fracture energy plotted against the average tensile bond strength. The latter is calculated by dividing the flexural bond strength by a factor 1.5, as suggested in literature [6]. Given the time-dependent relationship of flexural bond strength highlighted in Sect. 4, results

obtained at different ages are considered representative of different masonry types. The data set herein obtained was expanded by considering experimental results available in literature of both flexural type and direct tensile tests performed on different masonry and specimen types. Among these, direct tensile tests performed by Van der Pluijm [6], Sandoval [33] and Lizárraga [34] on couplets, four-point bending tests performed by Jafari [3] on wallets and four-point bending tests performed by Van der Pluijm [6] on stack-bonded prisms were considered in addition to a set of bond wrench tests performed by Licciardello et al. [35] with the CMOD-controlled set-up herein presented. Detailed information regarding the expanded data set herein considered is reported in Appendix A.

The results obtained in this study are in line with those obtained from other flexural tests reported by Jafari [3] and Van der Pluijm [6, 18]. Comparing both analysed parameters, the bond fracture energy was approximately one order of magnitude smaller than the tensile bond strength and showed a larger variability (C.o.V. ranging between 45 and 89%).

Comparing the results determined in flexural and direct tension tests, it can be observed that the fracture energy assessed through flexural type tests tends to be higher than the one evaluated through direct tensile tests. In particular, a factor of around 4 is obtained from the trend of the two data set herein considered.

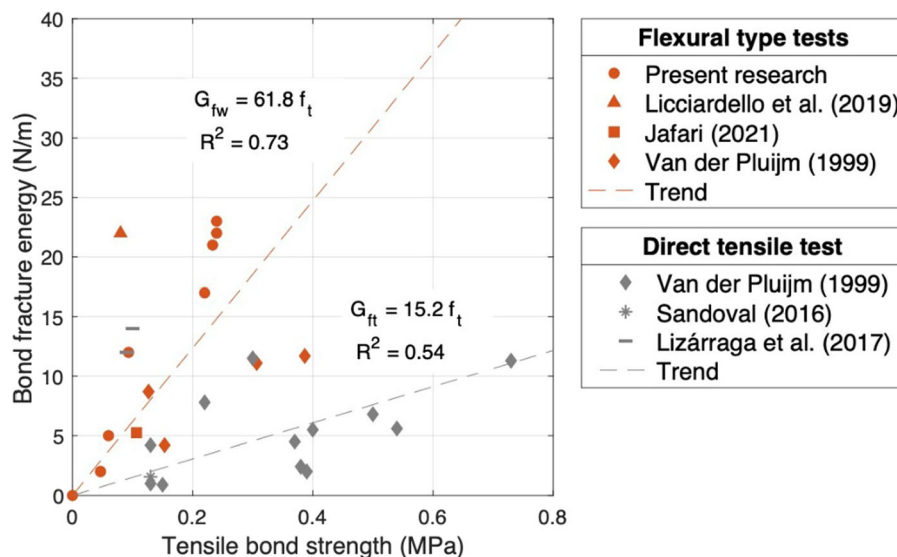


Fig. 6 Bond fracture energy evaluated through flexural type and direct tensile tests plotted against the tensile bond strength

This gap confirms the initial thoughts of Van der Pluijm [6] obtained by analysing a smaller data set. Given the complexity of capturing the post-peak behaviour in direct tensile test, limited data are available in literature. A more systematic study is therefore suggested to explore the reasons of this difference.

7 Conclusion

Through a comparative experimental approach, this study examined the influence of the set-up (manually-operated vs computer-controlled) and the specimen's type (with/without head joints and couplets vs wallet) on the flexural bond strength assessment using the bond wrench test. Among the set-ups considered, a procedure to evaluate the post-peak behaviour and assess the flexural bond fracture energy was also investigated. As a result, the following conclusions and recommendations can be drawn.

The accuracy and control of the bond wrench test set-up exhibited no influence on the flexural bond strength assessment. The three proposed set-ups provided a similar value of the coefficient of variation and, therefore, can be considered equivalent. Despite the manual control of the load, the portable set-up for in-situ applications is considered sufficient to determine a reliable result; consequently, the high variability observed in bond wrench test results is to be considered an intrinsic property of masonry. For laboratory applications, the CMOD-controlled configuration is suggested, because its implementation allows the assessment of the complete flexural bond behaviour in terms of both flexural bond strength and flexural bond fracture energy.

This study also confirms the specimen's type as an influencing factor affecting the masonry flexural bond strength assessment: the mean strength of "standard" stack-bonded couplets resulted significantly lower than the mean flexural bond strength of running-bonded wallets. Unlike several-brick high prisms tested by Correa et al. [12], couplets were found to underestimate the flexural bond strength of entire wallets. Therefore, couplets are suggested for design and control purposes among the specimen types suggested by the standard EN 1052-5:2002 [1]. To correlate laboratory tests performed on stack-bonded couplets to in-situ measurements, a different factor

was computed for CS and clay masonry, i.e., 1.5 and 2.2, respectively. Nevertheless, since limited experiments were performed, further research would be needed to confirm the established correlation factors and give more insight on the causes of this difference. Considering the lack of spatial correlation found between bed joints within the wallet, this study suggests attributing the difference to the presence of head joints which could modify the drying process of the specimen. Though, no consistent results for the two masonry types were obtained from running-bonded couplets and wallets that can confirm this aspect.

In addition to the specimen's type, the role played by the brick's absorption properties, mortar composition and hardening time on the development of flexural bond strength was corroborated. In particular, the brick's absorption properties, herein quantified through the initial rate of absorption, emerged as the primary contributor to the difference in flexural bond strength between the two types of masonry considered. This emphasizes the importance of considering the suction properties of bricks and evaluating if pre-wetting prior to construction is required to achieve a stronger bond in practical applications. On the other hand, the evolution of the flexural bond strength over time appeared to be strongly influenced by the mortar composition, particularly by the presence of lime. Unlike cement-based mortars, lime carbonation in specimen cast with the cement-lime mortar led to a progressive increase of strength within the period considered, i.e., from 4 to 197 days. This confirms that for masonry built with lime mortars, longer hardening time than 28 days are required to estimate the actual flexural bond strength.

Eventually, a procedure to determine the flexural bond fracture energy from laboratory bond wrench tests is also presented in this study. Such a procedure could be of crucial relevance if an accurate correlation with tensile bond fracture energy is assessed. For this purpose, a new crack-mouth opening controlled set-up is presented to measure the post-peak response. The set-up provides results that are in line with other type of flexural tests, i.e. four-point bending tests on wallets and stack-bonded prisms. By comparing results of flexural and direct tensile tests, a factor 4 was computed to correlate the flexural bond fracture energy to the tensile fracture energy. Although a difference might be expected due to the different



boundary conditions implemented and the state of stress to which the bed joint is subjected, a more systematic study is suggested to extend the data set to explore and validate the difference obtained.

Acknowledgements Part of this research was funded by Nederlandse Aardolie Maatschappij (NAM), under Contract No. UI67339 ‘Damage sensitivity of Groningen masonry building structures—Experimental and computational studies’ (contract holders: Jan van Elk and Jeroen Uilenreef), which is gratefully acknowledged. Part of the first author’s work was supported by a scholarship from the Polytechnic University of Turin. The authors are thankful to the staff of the TU Delft Macrolab/Stevinlaboratory and Edwin Meulman for the laboratory support and to Dr. Caspar Groot for discussions on water absorption and bond strength behaviour.

Open Access This article is licensed under a Creative Commons Attribution 4.0 International License, which permits use, sharing, adaptation, distribution and reproduction in any medium or format, as long as you give appropriate credit to the original author(s) and the source, provide a link to the Creative Commons licence, and indicate if changes were made. The

images or other third party material in this article are included in the article’s Creative Commons licence, unless indicated otherwise in a credit line to the material. If material is not included in the article’s Creative Commons licence and your intended use is not permitted by statutory regulation or exceeds the permitted use, you will need to obtain permission directly from the copyright holder. To view a copy of this licence, visit <http://creativecommons.org/licenses/by/4.0/>.

Data availability The experimental results of the presented tests and detailed pictures of the set-ups are available via the 4TU.ResearchData repository at <https://doi.org/10.4121/20193173>. The data are distributed under the license type CC BY.

Appendix A

An overview of the extended dataset, used in Sect. 6, is presented in Table 7. While direct tensile tests results are directly reported in terms of tensile bond

Table 7 Extended dataset to correlate bond fracture energy obtained through flexural type and direct tensile tests

References	Brick-mortara type		Flexural bond strength		Tensile bond strength		Bond fracture energy		Success rate
			Avg. (MPa)	C.o.V. (%)	Avg. (MPa)	C.o.V. (%)	Avg. (N/m)	C.o.V. (%)	
<i>Flexural test</i>									
Present research	Clay	1:2:9 ¹	0.14	37	0.09		12	86	10/10
			0	–	0.00		0	–	10/10
			0.07	40	0.05		2	59	10/10
			0.09	42	0.06		5	89	10/10
	CS	1:3 ²	0.33	7	0.22		17	46	10/10
			0.35	23	0.23		21	45	10/10
			0.36	29	0.24		23	61	10/10
			0.36	10	0.24		22	46	10/10
Licciardello et al. [35]	Clay	1:2:9 ¹	0.12	60	0.08		22	90	10/10
Jafari [3]	Clay	1:2:9 ¹	0.16	22	0.11		5.25	97	5/5
Van der Pluijm [6]	Soft mud clay (sm-RIJ)	1:1:6 ¹	0.19	37	0.13		8.7	65	3/4
	Wire cut clay (wc-JO9)	1:1:6 ¹	0.58	34	0.39		11.7	77	17/17
	CS (CS-brick90)	1:1:6 ¹	0.23	41	0.15		4.2	48	2/5
	Concrete (MBI)	fmGPM ³	0.46	16	0.31		11.1	38	5/5
<i>Direct tensile test</i>									
Van der Pluijm [6]	Soft mud clay (sm-VE)	1:2:9 ¹			0.22	60	7.8	65	4/5
	Soft mud clay (sm-VE)	1: ½:4½ ¹			0.13	101	4.2	32	3/3
	Wire cut clay (wc-JO9O)	1:2:9 ¹			0.30	24	11.5	64	3/3
	Wire cut clay (wc-JO9O)	1:1:6 ¹			0.40	39	5.5	70	27/33
	Wire cut clay (wc-JO9O)	1: ½:4½ ¹			0.50	29	6.8	51	6/6



Table 7 continued

References	Brick-mortara type	Flexural bond strength		Tensile bond strength		Bond fracture energy		Success rate
		Avg. (MPa)	C.o.V. (%)	Avg. (MPa)	C.o.V. (%)	Avg. (N/m)	C.o.V. (%)	
	Wire cut clay (wc-JO9O)	1:2:9 ¹		0.54	33	5.6	53	9/15
	Wire cut clay (wc-JO9O)	1:2:12 ¹		0.37	33	4.5	37	6/7
	Wire cut clay (wc-JO9O)	1:2:9 ¹		0.15	51	0.9	44	6/12
	Wire cut clay (wc-JO9O)	1:2:12 ¹		0.39	44	2.0	52	6/6
	Wire cut clay (wc-JO9O)	1:1:6 ¹		0.38	26	2.4	38	6/6
	Wire cut clay (wc-JO9O)	1:1:6 ¹		0.24	60	1.7	92	17/20
	Wire cut clay (wc-JO9O)	1:1:6 ¹		0.13	66	1.0	71	17/19
CS	1:2:9 ¹		0.32	34	–	–	0/4	
CS	1:1:6 ¹		0.33	51	–	–	0/5	
Concrete (MBI)	fmGPM ³		0.73	19	11.3	–	1/5	
Sandoval [33]	Perforated clay	fmGPM ³		0.13	20	1.6	37	3/3
Lizárraga et al. [34]	Perforated concrete	fmGPM ³		0.10	18	14	3	3/?
		1:¼:3 ¹		0.09	39	12	35	2/?

^aMortar composition by volume ratio: ¹cement:lime:sand or ²cement:lime/³fmGPM: factory made general purpose mortar

strength, flexural type tests results are reported in terms of both the measured flexural bond strength and the derived tensile bond strength. Each set's masonry type is indicated by specifying the brick–mortar type; the original code used by the author is also reported where available. Eventually, the success rate intended as the number of specimens successfully tested over the set size is reported.

References

- CEN (2005) EN 1052-5. Method of test masonry—part 5: determination of bond strength by bond wrench method. European Committee for Standardisation, Brussels
- ASTM Standard C1072 (2019) Standard test methods for measurement of masonry flexural bond strength. ASTM International, West Conshohocken
- Jafari S (2021) Material characterisation of existing masonry: a strategy to determine strength, stiffness and toughness properties for structural analysis. Delft University of Technology: TU Delft Applied Mechanics. <https://repository.tudelft.nl> Doctoral thesis
- Van der Pluijm R (1996) Measuring of bond: A comparative experimental research. In: 7th North American Masonry Conference, South Bend, IN, USA, 2–5 June 1996
- Zhou Z, Walker P, D' Ayala D (2008) Strength characteristics of hydraulic lime mortared brickwork. Proc Inst Civ Eng Constr Mater 161(4):139–146
- Van der Pluijm R (1999) Out-of-plane bending of masonry: behaviour and strength. PhD-Thesis, Technische Universiteit Eindhoven, Eindhoven
- De Vekey R, Page A, Hedstrom E (1994) Variability of bond wrench measurements in UK Australia and USA. Mason Int 8(1):21–25
- Baker L (1982) Some factors affecting the bond strength of brickwork. In: Wintz JA, Yorkdale AH (eds) Proceedings of 5th International Brick Masonry Conference (VIBMaC) held in Washington, DC, 5–10 Oct., 1979. McLean, Virginia
- Lawrence SJ, Page AW (1994) Bond studies in masonry. In: 10th international brick/block Masonry conference, 5–7 July, 1994; Calgary, Canada, pp 909–917. <http://hdl.handle.net/102.100.100/238303?index=1>
- Pavía S, Hanley R (2010) Flexural bond strength of natural hydraulic lime mortar and clay brick. Mater Struct 43(7):913–922
- Nichols JM, Holland NL (2011) A comparative study of balanced bond wrench testing and unbalanced bond wrench testing. Eleventh North American Masonry Conference, Minneapolis
- Corrêa MRS, Masia MJ, Stewart MG, Heffler LM (2012) An experimental and statistical analysis of the flexural bond strength of masonry walls. Aust J Struct Eng 13(2):139–148
- Chang LZ, Rots JG, Esposito R (2021) Influence of aspect ratio and pre-compression on force capacity of unreinforced masonry walls in out-of-plane two-way bending. Eng Struct 249:113350
- Zeng B, Li Y, Noguez CC (2021) Modeling and parameter importance investigation for simulating in-plane and out-of-plane behaviors of un-reinforced masonry walls. Eng Struct 248:113233



15. Celano T, Argiento LU, Ceroni F, Casapulla C (2021) In-plane behaviour of masonry walls: numerical analysis and design formulations. *Materials* 14(19):5780
16. Giardina G, Rots JG, Hendriks MAN (2013) Modelling of settlement induced building damage. TU Delft, Delft
17. Barros JA, Almeida JC, Lourenço PB (2002) Characterization of brick and brick–mortar interface under uniaxial tension. In: VII International seminar on structural masonry for developing countries. Belo Horizonte, Brasil
18. Van der Pluijm R (1997) Non-linear behaviour of masonry under tension. *HERON-ENGLISH EDITION* 42:25–54
19. NEN (2020) NPR 9998. Assessment of structural safety of buildings in case of erection, reconstruction and disapproval induced earthquakes: basis of design, actions and resistances. Nederlands Normalisatie-instituut, Delft
20. Khalilpour S, BaniAsad E, Dehestani M (2019) A review on concrete fracture energy and effective parameters. *Cem Concr Res* 120:294–321
21. Jafari S, Panoutsopoulou L, Rots JG (2015) Tests for the characterisation of original Groningen masonry. Delft University of Technology. Final report, 18
22. Safety assessment. (n.d.). TU Delft. <https://www.tudelft.nl/citg/structural-response-to-earthquakes/publications/safety-assessment>
23. CEN (2015) EN 772-1. Methods of test for masonry units—part 1: determination of compressive strength. European Committee for Standardisation, Brussels
24. CEN (2011) EN 772-11. Methods of test for masonry units—part 11: determination of water absorption of aggregate concrete, manufactured stone and natural action and the initial rate of water absorption of clay masonry units. European Committee for Standardisation, Brussels
25. CEN (1999) EN 1015-3. Methods of test for mortar for masonry—part 3: determination of consistence of fresh mortar (by flow table). European Committee for Standardisation, Brussels
26. CEN (2019) EN 1015-11. Methods of test for mortar for masonry—part 11: determination of flexural and compressive strength of hardened mortar. European Committee for Standardisation, Brussels
27. Korswagen P, Longo M, Meulman E (2019) Damage sensitivity of Groningen masonry structures—Experimental and computational studies—Stream 2: Part 1. Report number C31B69WP0–14, Report, version 1.0, 26 of June 2019
28. Gaggero MB (2019) Comparison of test methods to determine masonry bond flexural strength. Master's thesis, Polytechnic University of Turin
29. Sugo H, Page AW, Lawrence S (2007) Influence of age on masonry bond strength and mortar microstructure. *Can J Civil Eng* 34(11):1433–1442
30. CEN (2005) EN 1996-1-1. Eurocode 6: design of masonry structures—part 1–1: general rules for reinforced and unreinforced masonry structures. European Committee for Standardisation, Brussels
31. Heffler LM, Stewart MG, Masia MJ, Correa MRS (2008) Statistical analysis and spatial correlation of flexural bond strength for masonry walls. *Masonry Int* 21(2):59–70
32. Ghiassi B, Vermelfoort A, Lourenço PB (2019) Masonry mechanical properties. Numerical modeling of masonry and historical structures. Elsevier, Amsterdam, pp 239–261
33. Sandoval C, Arnau O (2017) Experimental characterization and detailed micro-modeling of multi-perforated clay brick masonry structural response. *Mater Struct* 50(1):1–17
34. Lizárraga JF, Pérez-Gavilán J (2017) Parameter estimation for nonlinear analysis of multi-perforated concrete masonry walls. *Constr Build Mater* 141:353–365
35. Licciardello L, Esposito R (2019) Material tests for the characterisation of replicated solid clay brick masonry. Delft University of Technology. Report number C31B04-WPC-2.3, version 3, 7 October 2019

Publisher's Note Springer Nature remains neutral with regard to jurisdictional claims in published maps and institutional affiliations.

